

## Another Look at Magic-Angle-Detected Fluorescence and Emission Anisotropy Decays in Fluorescence Microscopy

Jacek J. Fisz<sup>†</sup>

*Institute of Physics, Nicolaus Copernicus University, ul. Grudziadzka 5/7, PL 87-100 Toruń, Poland*

*Received: September 20, 2007; In Final Form: November 1, 2007*

It is shown that in contrast to a traditional fluorescence spectroscopy with the parallel beams of light, in which the kinetic fluorescence decays are collected at the so-called magic-angle of  $\theta_{\text{mag}} = 54.7^\circ$ , in the fluorescence microscopy, the value of the magic-angle depends on the numerical aperture (NA) of a microscope objective and on the refractive index ( $n$ ) of an immersion liquid used. Two methods enabling the determination of the magic-angle values corresponding to different values of NA/ $n$ , are discussed. It is shown that  $\theta_{\text{mag}}$  changes from a value of  $54.7^\circ$  at the  $\text{NA}/n \rightarrow 0$ , to a value of  $45^\circ$  with  $\text{NA}/n \rightarrow 1$ . Also in contrast to a traditional fluorescence spectroscopy, in the fluorescence microscopy the term  $I_{||}(t) + 2I_{\perp}(t)$  does not represent the total fluorescence intensity  $I_{\text{tot}}(t)$ , because the resulting fluorescence decay  $I_{||}(t) + 2I_{\perp}(t)$  is contributed by the dynamic evolution of excited fluorophores. A correctly defined total fluorescence intensity solely represents the kinetic evolution of excited fluorophores, and in the fluorescence microscopy it equals  $I_{\text{tot}}(t) = 3I_{\text{mag}}(t)$ , where  $I_{\text{mag}}(t)$  represents the fluorescence intensity detected at  $\theta_{\text{mag}}$  corresponding to a particular NA/ $n$  value. If the correct (true) decay of  $I_{\text{tot}}(t)$  is substituted into the denominator in the expression for the emission anisotropy  $r(t)$ ,  $r(t)$  is a (multi)exponential function of time and it accounts for the high-aperture excitation-detection conditions.

Fluorescence lifetime imaging (FLIM), single-molecule FLIM (smFLIM), Förster resonance energy transfer (FRET), single-pair FRET (spFRET), emission anisotropy imaging (EAIM), and single-molecule EAIM (smEAIM), are the spectroscopic techniques playing a key role in the fluorescence microscopy studies in many areas of medical and life sciences, and also in the field of nano(bio)technology. These examples of the very advanced applications of the fluorescence microscopy indicate that possibly most accurate description of this experimental technique is very desired to ensure a reliable and very precise analysis of the time-resolved and steady-state-excitation fluorescence microspectroscopy experimental data.

In our very recent article<sup>1</sup> we have discussed three treatments of the fluorescence microscopy. First, we introduced a description of this technique, in which the high-aperture excitation and detection processes are both considered in terms of the method based on the meridional plane properties (MPP) of the objective lenses.<sup>2,3</sup> Second, we proposed an approach which combines the high-aperture excitation treated within the diffraction theory,<sup>2–5</sup> with the high-aperture detection considered within the MPP-based method. Both descriptions lead to identical formulas with differently defined coefficients representing the high-aperture excitation process. Third, by combining the reference fluorophore method<sup>6</sup> with the general (symmetry adapted) description of the fluorescence polarization spectroscopy of macroscopically isotropic molecular media,<sup>1</sup> we outlined a calibration method enabling the analysis of all (far-field) fluorescence polarization experiments performed on arbitrarily

complicated instruments, without the necessity of derivation of the explicit expressions for polarized fluorescence decays corresponding to a particular experimental case of interest.

The MPP-based description of the fluorescence polarization microscopy is given by very simple mathematical formulas that enable one to immediately display all basic properties of this spectroscopic technique. We have employed this description to examine: (a) the properties of the total fluorescence decay  $I_{\text{tot}}(t, \alpha_0)$ , defined traditionally by

$$I_{\text{tot}}(t, \alpha_0) = I_{||}(t, \alpha_0) + 2I_{\perp}(t, \alpha_0) \quad (1)$$

(b) the properties of the magic-angle-detected fluorescence decay  $I_{\text{mag}}(t, \alpha_0)$ , detected traditionally at the so-called magic-angle  $54.7^\circ$  (and which holds the equality  $I_{\text{tot}}(t, \alpha_0) = 3I_{\text{mag}}(t, \alpha_0)$ <sup>1</sup>), and (c) the properties of the emission anisotropy decay  $r(t, \alpha_0)$  defined traditionally by

$$r(t, \alpha_0) = \frac{I_{||}(t, \alpha_0) - I_{\perp}(t, \alpha_0)}{I_{\text{tot}}(t, \alpha_0)} = \frac{I_{||}(t, \alpha_0) - I_{\perp}(t, \alpha_0)}{3I_{\text{mag}}(t, \alpha_0)} \quad (2)$$

In the above equations  $\alpha_0$  is the cone half-angle of an microscope objective and  $\alpha_0 = \arcsin(\text{NA}/n)$ , where NA is the numerical aperture of the objective and  $n$  is the refractive index of an immersion liquid.

The decays  $I_{\text{tot}}(t, \alpha_0)$ ,  $I_{\text{mag}}(t, \alpha_0)$ , and  $r(t, \alpha_0)$ , defined as mentioned before, are commonly used in the literature in the fluorescence microscopy studies in all of the above-mentioned applications. Furthermore, by a correspondence to traditional fluorescence spectroscopy,  $I_{\text{tot}}(t, \alpha_0)$  and  $I_{\text{mag}}(t, \alpha_0)$  are usually

<sup>†</sup> E-mail: jjfisz@phys.uni.torun.pl.

assumed to solely represent the kinetic fluorescence decay, i.e.,  $I_{\text{tot}}(t, \alpha_0) = I_{||}(t, \alpha_0) + 2I_{\perp}(t, \alpha_0) = 3I_{\text{mag}}(t, \alpha_0) \sim \text{Ph}(t)$ , and  $r(t, \alpha_0)$  is usually assumed to be a (multi)exponential function of time, i.e.,  $r(t, \alpha_0) = 0.4W(t)$ . Here  $\text{Ph}(t)$  represents the kinetic fluorescence decay and  $W(t)$  means the rotational diffusion correlation function. However, as was shown in ref 1, when the high-aperture excitation-detection conditions are taken into account, the explicit expressions for  $I_{\text{tot}}(t, \alpha_0)$  and  $I_{\text{mag}}(t, \alpha_0)$  are described by

$$\begin{aligned} I_{\text{tot}}(t, \alpha_0) &= I_{||}(t, \alpha_0) + 2I_{\perp}(t, \alpha_0) = \\ &3I_{\text{mag}}(t, \alpha_0) \sim \text{Ph}(t) + c_{\text{tot}}(\alpha_0) W(t) \text{ Ph}(t) \end{aligned} \quad (3)$$

and which evidently demonstrates that neither  $I_{\text{mag}}(t, \alpha_0)$  nor  $I_{||}(t, \alpha_0) + 2I_{\perp}(t, \alpha_0)$  solely represent the kinetic fluorescence decays because of a clear contribution of the kinetic-dynamic term  $W(t) \text{ Ph}(t)$ . The contribution of  $W(t) \text{ Ph}(t)$  depends on the value of the coefficient  $c_{\text{tot}}(\alpha_0) = 1/5(R_0(\alpha_0) Q_0(\alpha_0) - R_2(\alpha_0) Q_2(\alpha_0))$ .<sup>1</sup> The coefficients  $R_p(\alpha_0)$  and  $Q_p(\alpha_0)$  describe the effects of the high-aperture excitation and detection, respectively, and they are given explicitly in ref 1. Furthermore, as a natural consequence of eq 3, at the high-aperture excitation and/or detection, the emission anisotropy  $r(t, \alpha_0)$  defined by eq 2, is described by<sup>1</sup>

$$r(t, \alpha_0) = 0.4 \frac{R_2(\alpha_0) Q_2(\alpha_0) W(t)}{1 + c_{\text{tot}}(\alpha_0) W(t)} \quad (4)$$

and which is a nonexponential function of time. Denoting by  $r_p(t) = 0.4W(t)$  the emission anisotropy that would be obtained from a traditional experiment with the parallel beams of light, eq 4 and the corresponding expression for a steady-state excitation can be written as

$$r(t, \alpha_0) = \frac{c_r(\alpha_0) r_p(t)}{1 + 5/2c_{\text{tot}}(\alpha_0) r_p(t)} \quad \bar{r}(\alpha_0) = \frac{c_r(\alpha_0) \bar{r}_p}{1 + 5/2c_{\text{tot}}(\alpha_0) \bar{r}_p} \quad (5)$$

where  $c_r(\alpha_0) = R_2(\alpha_0) Q_2(\alpha_0)$  is the high-aperture excitation-detection proportionality coefficient for the emission anisotropy. As was mentioned already in ref 1, the contribution of the kinetic-dynamic term to the evolution of total fluorescence intensity decay was encountered earlier by Axelrod<sup>5</sup> for a parallel-beam excitation and high-aperture detection experimental conditions.

Although from the mathematical point of view eqs 3–5 correctly describe the time evolution of the decays  $I_{\text{tot}}(t, \alpha_0)$ ,  $I_{\text{mag}}(t, \alpha_0)$ , and  $r(t, \alpha_0)$  at the high-aperture excitation and/or detection (when they are calculated according to eqs 1 and 2), from the physical point of view these equations do not display the properties that  $I_{\text{tot}}(t, \alpha_0)$ ,  $I_{\text{mag}}(t, \alpha_0)$ , and  $r(t, \alpha_0)$  should exhibit according to their definitions; namely, (a)  $I_{\text{tot}}(t, \alpha_0)$  and  $3I_{\text{mag}}(t, \alpha_0)$  mean the overall fluorescence intensity and, hence, should solely represent the kinetic decay of fluorescence, and (b) the denominator in eq 4 should not be dependent on rotational dynamics of photoselected fluorophores because  $r(t, \alpha_0)$  represents the anisotropy of emitted fluorescence normalized with respect to the fluorescence signal proportional to the number density of all fluorophores emitting the fluorescence. Furthermore, from the experimental point of view, eq 3 suggests that the photophysical properties of fluorophores cannot be determined without considering their rotational dynamics. It is clear, therefore, that the definitions of  $I_{\text{mag}}(t, \alpha_0)$ ,  $I_{\text{tot}}(t, \alpha_0)$ , and  $r(t, \alpha_0)$ , taken directly from the traditional fluorescence spectroscopy

with the parallel beams of the exciting light and collected fluorescence (eqs 1 and 2), do not apply to fluorescence microscopy, and to the fluorescence spectroscopy with the objective lenses, in general.

In addition to what has been outlined and discussed in our very recent article,<sup>1</sup> we here want to demonstrate a treatment to the problem of the magic-angle-detected and total fluorescence decays for the fluorescence microscopy, in which, first,  $I_{\text{mag}}(t, \alpha_0)$  and  $I_{\text{tot}}(t, \alpha_0)$  will exhibit the before mentioned properties, and second, when correctly defined decay  $I_{\text{tot}}(t, \alpha_0)$  is substituted into the denominator of eq 2, the decay of the emission anisotropy  $r(t, \alpha_0)$  will exhibit a correct time dependence.

The intensity of polarized fluorescence decay detected at an arbitrary angle of polarization direction  $\theta_f^{(0)}$  can be described by a general (symmetry adapted) formula (6)

$$I(t, \alpha_0, \theta_f^{(0)}) \sim \text{Ph}(t) + K(\alpha_0, \theta_f^{(0)}) W(t) \text{ Ph}(t) \quad (6)$$

(see ref 1 for details), where the factor  $K(\alpha_0, \theta_f^{(0)})$ , describing the contribution of the kinetic-dynamic term  $W(t) \text{ Ph}(t)$ , depends on the cone half-angle  $\alpha_0$  and on the detection angle  $\theta_f^{(0)}$ . The magic-angle condition, which means from the physical point of view that the detected fluorescence decay solely depends on the photophysical decay  $\text{Ph}(t)$ , implies a mathematical condition given by

$$K(\alpha_0, \theta_f^{(0)}) = 0 \quad (7)$$

The value of angle  $\theta_f^{(0)}$  that fulfills this condition represents the magic-angle value  $\theta_{f,\text{mag}}^{(0)}$  corresponding to a particular value of  $\alpha_0 = \arcsin(\text{NA}/n)$ . This means that in contrast to a traditional fluorescence spectroscopy, in the fluorescence microscopy there exist a “spectrum” of the magic angles, each corresponding to a particular value of the ratio  $\text{NA}/n$ , ranging from a value of  $\text{NA}/n \rightarrow 0$  to a value of  $\text{NA}/n \rightarrow 1$ .

For any fixed value of  $\text{NA}/n$ , condition 7 can be explored experimentally by employing a reference fluorophore in a solution phase of known decay parameters of its photophysics  $\text{Ph}_r(t)$ . By performing a few microscopic measurements on the reference fluorophore, at different  $\theta_f^{(0)}$ , one can establish the value of  $\theta_{f,\text{mag}}^{(0)}$  at which the analysis of the collected fluorescence decay  $I(t, \alpha_0, \theta_{f,\text{mag}}^{(0)})$  returns the decay parameters of  $\text{Ph}_r(t)$ . This method is purely empirical and it compensates for the possible experimental artifacts (e.g., a dichroic-mirror-induced modification of the polarization direction of the fluorescence detected, in the case of the fluorescence microscope depicted in Scheme 1a).

The magic-angle-condition 7 can also be considered within the MPP-based description of the fluorescence microscopy.<sup>1</sup> The explicit expression for  $K(\alpha_0, \theta_f^{(0)})$  can be found from

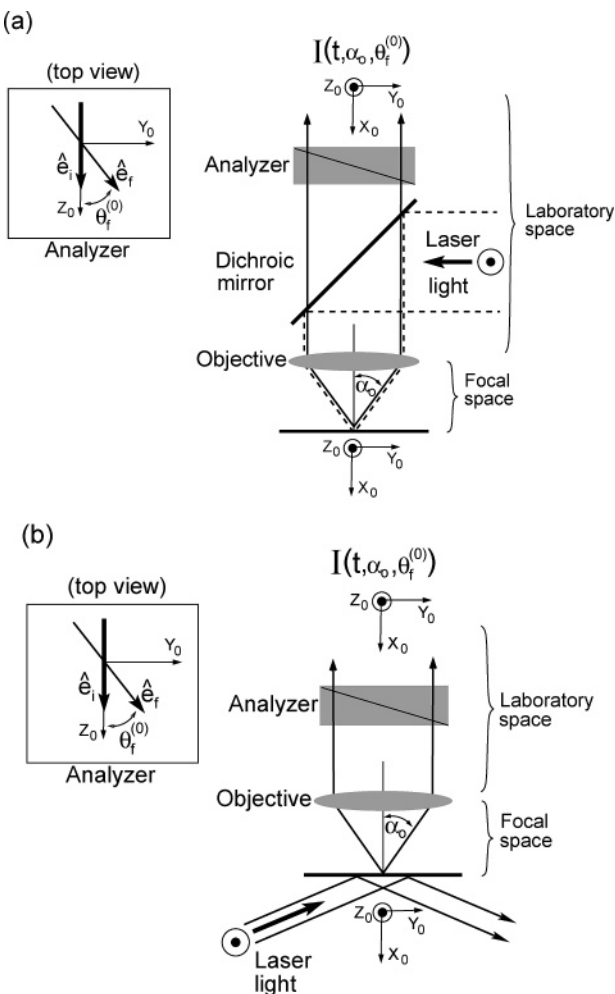
$$I(t, \alpha_0, \theta_{f,\text{mag}}^{(0)}) = I_{||}(t, \alpha_0) \cos^2 \theta_f^{(0)} + I_{\perp}(t, \alpha_0) \sin^2 \theta_f^{(0)} \quad (8)$$

after taking into account the explicit expressions for  $I_{||}(t, \alpha_0)$  and  $I_{\perp}(t, \alpha_0)$  given by eqs 56 and 57 of ref 1. Finally, the explicit form of  $K(\alpha_0, \theta_f^{(0)})$  is given by

$$K(\alpha_0, \theta_f^{(0)}) = \frac{1}{5}(3R_2(\alpha_0) Q_2(\alpha_0) \cos 2\theta_f^{(0)} + R_0(\alpha_0) Q_0(\alpha_0)) \quad (9)$$

and which is a simplified form of the same factor standing in eq 63 of ref 1. The magic-angle-condition 7 for  $K(\alpha_0, \theta_f^{(0)})$ ,

**SCHEME 1:** (a) Wide-Field and Confocal Fluorescence Microscope and (b) Evanescent-Wave-Excitation Fluorescence Microscope



given by the above expression, leads to

$$\theta_{f,\text{mag}}^{(0)} = \frac{1}{2} \arccos \left( -\frac{R_0(\alpha_0) Q_0(\alpha_0)}{3R_2(\alpha_0) Q_2(\alpha_0)} \right) \quad (10)$$

which describes the dependence of the magic-angle-value  $\theta_{f,\text{mag}}^{(0)}$  on the cone half-angle  $\alpha_0$ . In Figure 1a,b we show the plots of  $K(\alpha_0, \theta_f^{(0)})$ , for the fixed values of  $\alpha_0 = 0^\circ, 20^\circ, 40^\circ, 55^\circ$ , and  $70^\circ$ , for the wide-field and confocal fluorescence microscopy (Figure 1a) and for the evanescent-wave-excitation fluorescence microscopy (Figure 1b).

Scheme 1a represents a wide-field or confocal fluorescence microscope, in which the high-aperture excitation and detection are combined, i.e.,  $R_p(\alpha_0) < 1$  and  $Q_p(\alpha_0) < 1$ . Scheme 1b shows an evanescent-wave-excitation fluorescence microscope, which refers to a parallel-beam-excitation and high-aperture-detection case; hence  $R_p(\alpha_0) = 1$  and  $Q_p(\alpha_0) < 1$  (see ref 1 for details). In both cases of Scheme 1, the exciting light is polarized along the  $Z_0$  axis and the analyzer selects the desired polarization direction (i.e., a particular angle  $\theta_f^{(0)}$ ) of the fluorescence signal  $I(t, \alpha_0, \theta_f^{(0)})$ . The plots shown in Figure 1a,b display an evident variation of the magic-angle value  $\theta_{f,\text{mag}}^{(0)}$  with the change of  $\alpha_0$ . Figure 1c demonstrates the dependence of  $\theta_{f,\text{mag}}^{(0)}$  on  $\alpha_0$ , defined by eq 10. As seen from Figure 1c,  $\theta_{f,\text{mag}}^{(0)}$  changes from a value of  $54.7^\circ$  at  $NA/n \rightarrow 0$ , to a value of  $45^\circ$  with  $NA/n \rightarrow 1$ . Very interesting is the case of very-high-aperture excitation and

detection (VHA), that is when  $NA/n \rightarrow 1$ . At this limit  $\theta_{f,\text{mag}}^{(0)}$  is close to a value of  $45^\circ$ , and hence, eq 8 gives a decay of  $I_{\text{unp},\text{VHA}}(t) = I_{||,\text{VHA}}(t) + I_{\perp,\text{VHA}}(t) \sim Ph(t)$ , describing the  $Y_0Z_0$ -plane-unpolarized fluorescence decay, as was discussed in ref 1. The same result can be obtained after integrating eq 8 over  $\theta_f^{(0)}$ , namely  $I_{\text{unp},\text{VHA}}(t) = \int_0^{2\pi} I(t, \alpha_0, \theta_f^{(0)}) d\theta_f^{(0)} \sim I_{||,\text{VHA}}(t) + I_{\perp,\text{VHA}}(t)$ . This means that, if the dichroic mirror being placed in the detection channel of a microscope does not modify polarization of the fluorescence detected, the kinetic fluorescence decay can be detected at the VHA conditions without applying of any analyzer.

When the denominator in eq 2 is represented by the true total fluorescence decay,

$$I_{\text{tot}}(t, \alpha_0) = 3I(t, \alpha_0, \theta_{f,\text{mag}}^{(0)}) = 3C Ph(t) \quad (11)$$

where  $C$  is a constant, the time evolution of  $r(t, \alpha_0)$  is a (multi)-exponential function of time, as shown in

$$r(t, \alpha_0) = \frac{I(t, \alpha_0, 0^\circ) - I(t, \alpha_0, 90^\circ)}{3I(t, \alpha_0, \theta_{f,\text{mag}}^{(0)})} = 0.4R_2(\alpha_0) Q_2(\alpha_0) W(t) \quad (12)$$

where  $I(t, \alpha_0, 0^\circ)$  and  $I(t, \alpha_0, 90^\circ)$  are taken from ref 1 (eqs 56 and 57 therein) or, equivalently, they are calculated from eqs 6 and 9. Equation 12 leads to very important (from the experimental point of view) and very simple mathematical relationships between  $r(t, \alpha_0)$  and its steady-state value  $\bar{r}(\alpha_0)$ , on one hand, and the corresponding emission anisotropies  $r_p(t) = 0.4W(t)$  and  $\bar{r}_p = 0.4W Ph/Ph$  that would be obtained from the traditional experiments with the parallel beams of light, on the other hand, given by

$$r(t, \alpha_0) = c_r(\alpha_0) r_p(t) \quad \bar{r}(\alpha_0) = c_r(\alpha_0) \bar{r}_p \quad (13)$$

Notice that when the total fluorescence intensity is represented by the correctly detected decay, the relationship between  $r(t, \alpha_0)$  and  $r_p(t)$  is linear, in contrast to a strongly nonlinear one given by eq 5. In Figure 1d we show the plots of  $c_r(\alpha_0)$  for the case of a wide-field and confocal fluorescence microscopy (solid line), and for evanescent-wave-excitation fluorescence microscopy (dashed line).

The symmetry adapted formula 6 together with the magic-angle-condition 7 and with the application of the reference fluorophore method represents a general treatment to the problem of correctly defined total fluorescence intensity decay  $I_{\text{tot}}(t, \alpha_0)$  given by eq 11.  $I_{\text{tot}}(t, \alpha_0)$ , when substituted into the denominator of eq 2, leads to an expression for the emission anisotropy that displays the desired time evolution. This treatment concerns a general case of the fluorescence polarization experiments (e.g., with spherical or cylindrical objective lenses) on arbitrary macroscopically isotropic samples (solutions, solutions of labeled macromolecules or membrane vesicles suspension). Fluorescence polarization microscopy or traditional fluorescence polarization experiments are just two of the possible cases. When considering the explicit description of the fluorescence microscopy in terms of the MPP-based model, from the magic-angle-condition 7 we have obtained the explicit expression describing the dependence of  $\theta_{f,\text{mag}}^{(0)}$  on the cone half-angle  $\alpha_0 = \arcsin(NA/n)$ . The fluorescence decays detected at  $\theta_{f,\text{mag}}^{(0)}$  represent the kinetic decay of fluorescence, and they have to be substituted into the denominator of the emission anisotropy. In the zero-aperture limiting case, i.e., when  $NA/n \rightarrow 0$  (hence  $\alpha_0 \rightarrow 0$  and  $\theta_{f,\text{mag}}^{(0)} \rightarrow 54.7^\circ$ ), the expressions for

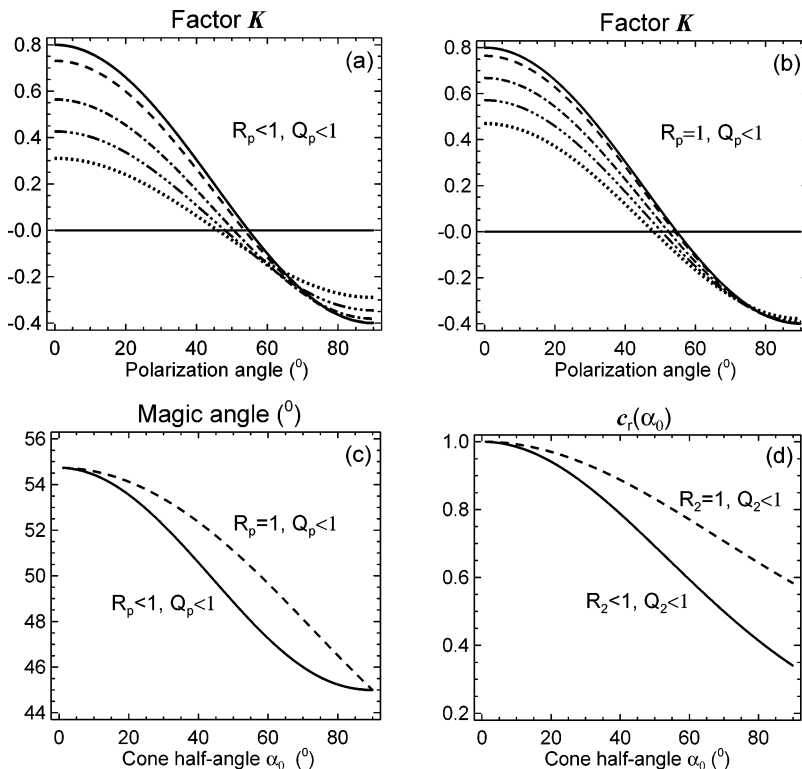


**Figure 1.** Plots of  $K(\alpha_0, \theta_f^{(0)})$ , for  $\alpha_0 = 0^\circ$  (—),  $20^\circ$  (---),  $40^\circ$  (-·-),  $55^\circ$  (-··-),  $70^\circ$  (···), for (a) a wide-field and confocal fluorescence microscopy and (b) an evanescent-wave-excitation microscope. (c) Dependence of  $\theta_{f,\text{mag}}^{(0)}$  versus  $\alpha_0$ . (d) Plots of  $c_r(\alpha_0)$  for a wide-field and confocal fluorescence microscope (solid line) and for an evanescent-wave-excitation fluorescence microscope (dashed line).

$I_{\text{tot}}(t, \alpha_0)$  and  $r(t, \alpha_0)$  become equivalent with the well-known corresponding ones,  $I_{\text{tot}}(t)$  and  $r_p(t)$ , describing the traditional fluorescence polarization experiments. Only in this very particular case does the equality  $I_{||}(t) + 2I_{\perp}(t) = 3I_{\text{mag}}(t)$  hold. It is clear, therefore, why the traditionally defined  $I_{\text{tot}}(t)$  and  $r_p(t)$  do not apply to the fluorescence polarization microscopy. Simply, the resulting decay  $I_{||}(t) + 2I_{\perp}(t)$  and magic-angle  $54.7^\circ$  do not define the general conditions for the total fluorescence intensity decay in this technique.

In principle, what has been discussed and described theoretically in our recent article,<sup>1</sup> was demonstrated much earlier experimentally in the excellent work by Keating and Wensel.<sup>7</sup> This paper was unknown to us when submitting the manuscript of ref 1. In their pioneering work on the use of the nanosecond fluorescence microscope in the studies of the kinetic and dynamic properties of fluorophores in the single cells, Keating and Wensel have noted that the application of the microscope objectives lead to much lower initial emission anisotropies  $r(t=0, \alpha_0)$  as compared to traditionally recovered ones  $r_p(t=0)$ . They have observed that when the microscope objective of 0.85 NA is replaced by another one of 1.3 NA, the initial anisotropy was reduced by 14–25%. Furthermore, from the traditional measurements for the fluorophore Fura-2 they obtained  $r_p(t=0) = 0.4$  (calculated from the data in Table 2 of ref 7, i.e.  $r_p(t=0) = \beta_1 + \beta_2$ ), but from the microscopic experiments for the same

fluorophore ( $\text{NA}/n = 0.884$ ; hence  $\alpha_0 \approx 62^\circ$ ) they obtained  $r(t=0, \alpha_0) \approx 0.25$  (according to Figure 5b of ref 7). It is also important to mention the case of macroscopic and microscopic picosecond fluorescence polarization measurements for the fluorophore *p*-terphenyl in a solution phase, reported in ref 6, and which demonstrate that the macroscopic value of emission anisotropy  $r_p(t=0) \approx 0.4$  is reduced to a value of  $r(t=0, \alpha_0) \approx 0.26$ , obtained from the microscopic measurements at  $\text{NA}/n = 0.856$  (hence  $\alpha_0 \approx 59^\circ$ ). All these observations are in excellent agreement with the values of  $r(t=0, \alpha_0)$  shown in Figure 3b of our work.<sup>1</sup> It is very likely, therefore, that the MPP-based method represents enough accurate description of the fluorescence microscopy technique.

## References and Notes

- (1) Fisz, J. *J. Phys. Chem. A* **2007**, *111*, 8606–8621.
- (2) Richards, B.; Wolf, E. *Proc. R. Soc. Lond. A. Math. Phys. Sci.* **1959**, *253*, 358–379.
- (3) Axelrod, D. *Biophys. J.* **1979**, *26*, 557–574.
- (4) Yoshida, A.; Asakura, T. *Optik* **1974**, *41*, No. 3, 281–292.
- (5) Axelrod, D. In *Fluorescence Polarization Microscopy*; Taylor, D. L., Wang, Y.-L., Eds.; Methods in Cell Biology, 30; Academic Press: New York, 1989; pp 333–352.
- (6) Koshioka, M.; Sasaki, K.; Masuhara, H. *Appl. Spectrosc.* **1995**, *49*, 224–228.
- (7) Keating, S. M.; Wensel, T. G. *Biophys. J.* **1991**, *59*, 186–202.